

A simple model describes the PDF of a non-graphitizing carbon

Michael A. Smith^a, Henry C. Foley^b, Raul F. Lobo^{a,*}

^a Colburn Laboratory, Department of Chemical Engineering, Center for Catalytic Science and Technology, University of Delaware, 150 Academy Street, Newark, DE 19716, USA

^b Fenske Laboratory, Department of Chemical Engineering, Penn State University, University Park, PA 16802, USA

Received 6 April 2004; accepted 7 April 2004

Available online 12 May 2004

Abstract

A model for the structure of a non-graphitizing carbon is built by randomly incorporating between 0.5% and 4% non-hexagonal rings into an extended sp^2 carbon sheet. The sheets are created using Cerius² Modeling software, optimized using a DREIDING force-field, and turbostratically layered to create a three-dimensional structure. We show that the calculated pair distribution function (PDF) for models containing approximately 1% non-hexagonal rings is remarkable similar to the experimental PDF obtained from neutron scattering by a non-graphitizing carbon prepared from polyfurfuryl alcohol pyrolyzed at 1200 °C. No attempt was made to fit the model to the experimental data, and the model has no adjustable parameters except for the fraction of non-hexagonal rings.

© 2004 Elsevier Ltd. All rights reserved.

Keywords: Non-graphitizing carbon; Modeling; Neutron scattering; Microstructure

1. Introduction

Non-crystalline forms of carbon are important industrial materials whose detailed structure has remained a scientific problem for over 50 years [1–6]. These materials are generally classified according to the manner of preparation, type of bonding (sp^2 or sp^3), and the hydrogen content [3]. Here we are concerned with non-graphitizing and glassy carbons formed by the pyrolysis of an appropriate precursor such as sucrose, polyvinylidene chloride, or as in this work, polyfurfuryl alcohol. Within this class, the materials resemble graphite in that they are sp^2 carbon, but unlike graphite they do not have long-range order and they are considered amorphous or disordered. The hydrogen content and degree of order depends upon the pyrolysis temperature. If pyrolysis is between 400 and 800 °C, the product has significant accessible microporosity [4]. These porous materials are called nanoporous carbons, and typically have a narrow, controllable pore size distribution between 4 and 20 Å. Nanoporous carbons

function as molecular sieves: their ability to separate molecules based on size and shape has rendered them useful in the chemical industry [4]. In contrast, materials produced at temperatures above 1200 °C contain essentially no accessible microporosity; these materials can no longer be defined as nanoporous and are better described as glassy carbons [3,5]. Disordered carbons are finding applications in lithium-batteries [7], and due to their hardness and chemical inertness, glassy carbons find use as electrodes [8].

Despite their utility, no satisfactory structural model has emerged that accounts for all the observed properties of these carbons. X-ray and neutron scattering experiments reveal that these materials have no structural order beyond 2 nm [3,4]. Images from high-resolution transmission electron microscopy (HRTEM) of both nanoporous and glassy carbons show a convoluted network of curved and layered domains with layer spacing of 4–5 Å, somewhat larger than the interlayer spacing of graphite (3.4 Å) [6,9]. The details of the local structure of non-graphitizing carbons are of paramount importance to understand the properties of these materials. In this paper we combine insights from HRTEM studies with PDF analysis to show that the curvature and correlation length seen in non-graphitizing carbons

* Corresponding author. Tel.: +1-302-831-1261; fax: +1-302-831-2085.

E-mail address: lobo@che.udel.edu (R.F. Lobo).

may be readily explained by constructing a model of carbon with a small fraction of non-hexagonal rings.

The local structure of amorphous (and crystalline) materials may be described by the pair distribution function, denoted $G(r)$ and given by [10,11]

$$G(r) = 4\pi r[\rho(r) - \rho_0]$$

where r is the radial distance separating atom pairs, $\rho(r)$ the atom number density and ρ_0 the average density. For model structures, the pair distribution function is calculated directly from

$$G(r) = \frac{1}{r} \sum_i \sum_j \left[\frac{f_i f_j}{\langle f \rangle^2} \delta(r - r_{ij}) \right] - 4\pi r \rho_0$$

Experimentally, the PDF may be obtained from X-ray, electron or neutron scattering measurements, where the measured reduced structure factor is related to the PDF by

$$G(r) = \frac{2}{\pi} \int_0^\infty Q \cdot [S(Q) - 1] \cdot \sin(rQ) dQ$$

Here, Q is the magnitude of the scattering vector, and $S(Q)$ is the reduced structure factor, each given by

$$Q = \frac{4\pi \sin(\theta)}{\lambda}$$

$$S(Q) = \frac{I_{\text{cu}}(Q)}{f^2}$$

The I_{cu} is the corrected scattering intensity given in electron units, N the number of atoms, and f the atomic scattering factor. Experimentally, there is an upper limit to the magnitude of the scattering vector Q , and the upper bound of the integral above is terminated at Q_{max} .

A number of investigators have proposed structural models for porous carbon materials based upon X-ray [2,8,12], electron [13] or neutron scattering data [7,14–16]. Warren [1] showed the orientations of layered graphite domains in heat-treated carbon blacks are uncorrelated, and described this translationally-disordered, layered arrangement as turbostratic. Franklin observed that all non-graphitic carbons have a turbostratically layered-structure fraction, and showed non-graphitizing carbons could be described as composed of small microdomains of graphene sheets [2]. Conceptually these observations are the basis for many subsequent models of disordered sp^2 carbons. For example, Thompson and Gubbins [12] used a reverse Monte Carlo technique to fit the size and arrangement of graphene sheets in the model structure to an experimental pair distribution function obtained by small-angle X-ray scattering. More recently, Claye and Fisher [7] employed this same concept of limited microdomains of graphene sheets in their study of lithium placement in non-graphitizing carbons; they point out that the hydrogen content and electron spin density in real

nanoporous carbons is not consistent with the significant number unfilled vacancies at the edge of the graphene microdomains in such models. Review articles summarizing these models successes and limitations (see Foley et al. [17] or Harris [5]) are available.

Pulsed neutron sources afford the highest resolution data available. Burian et al. [15] used this technique to measure the PDF of a non-graphitizing carbon produced from phenol formaldehyde resin and concluded there is a separation of single and double bond character within the graphene sheets. Petkov et al. [16] measured the pair distribution function of three samples of carbon prepared from polyfurfuryl alcohol. To optimize their model, they displaced the atoms in a graphene sheet, and through this approach were able to fit the experimental data reasonably well. No rationale as to the physical basis for the perturbations—atomic dislocations, atom vacancies, and graphene sheet curvature—was given. However, Petkov's neutron scattering study remains the best available data set for these materials and we will use these data as the basis for our investigations (see Fig. 1).

Additional information on the structure of carbon has been obtained using high-resolution transmission electron microscopy. Harris and Tsang [9] obtained images of glassy carbons that reveal onion-like structures much like those seen in the co-products of fullerene and nanotube synthesis, and suggested the observed curvature in non-graphitizing carbons is due to the existence of 5-member rings in the carbon sheets. Others have proposed hypothetical structures with negative curvature—the so called Schwarzites—based on the existence of 7-member rings [18–21]. Bourgeois and

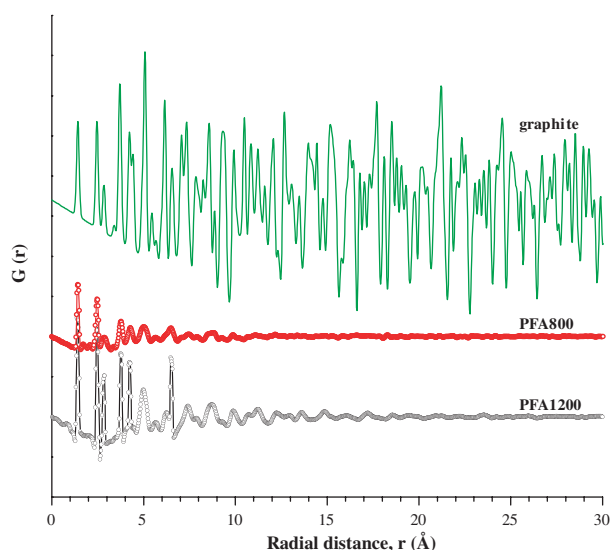


Fig. 1. Atomic pair distribution functions (PDF) from a graphite model, and experimental PDF of non-graphitizing carbons prepared from polyfurfuryl alcohol pyrolyzed at 800 and 1200 °C, materials designated as PFA800 and PFA1200 respectively.

Bursill [22] have also identified negatively curved sheets in HRTEM images of glassy carbon.

In this paper, following the observations from HRTEM studies cited above, we build a 3-D model using a two-dimensional, sp^2 carbon building unit where most of the carbon in the expected hexagonal tiling arrangement. However, we also incorporate a small fraction of randomly placed non-hexagonal rings while still maintaining the sp^2 configuration; these non-hexagonal rings result in curved structures. After the geometry of the 2D building unit is optimized, a 3D structure is created by turbostratically layering the curved layers, and the model PDF is calculated and compared to experimental PDF of Petkov et al. [16]. This approach is distinct from other attempts to fit graphene-like structures to the PDF by geometrically altering the positions of individual carbon atoms (i.e., geometric perturbations) and instead uses ‘topological’ perturbations to generate new model structures. Results show that this approach generates structures with a PDF that closely resemble the experimental PDF of non-graphitizing carbons with no adjustable parameters except for the fraction of non-hexagonal rings.

2. Materials and model

The PDFs of Fig. 1 were obtained from two samples prepared from pyrolysis of polyfurfuryl alcohol at temperatures of 800 and 1200 °C. The materials prepared at 800 °C have a density of 1.72 g cm⁻³ [16], and a H/C molar ratio of 0.10 [4]. This material was prepared at the upper end of the temperature range where useful microporosity is expected to exist, and is designated PFA800. The material prepared at 1200 °C has a density of 2.2 g cm⁻³, and an expected H/C ratio of 0.03. We designate this as PFA1200. Both samples are assumed to be composed solely of carbon and hydrogen [17].

Model structures of a single carbon sheet were created using the Cerius² [23] simulation package operating

on a Silicon Graphics Indigo2 ® with an IRIX 6.3 operating system. Cerius² provides a suitable but not necessarily unique molecular modeling software platform from which to systematically build these amorphous carbon layers. Individual layers were formed by adding carbon atoms to the edges of a benzene or a pyrene molecule stripped of hydrogen. All the carbon atoms have a sp^2 electronic configuration. The atoms were added preserving the hexagonal atomic arrangement, except that disorder in the connectivity was incorporated by randomly adding a 5- or 7-member ring. These 5- and 7-rings forced curvature in the overall sheet, forming cusps and saddles respectively. All the carbon rings adjacent to a 5- or 7-member ring were forced to be hexagonal. A single sheet was grown by successively adding carbons up to a total of 1200–2000 atoms. Linear dimensions of the sheets of about 50 × 50 Å are typical. Construction of individual sheets was an iterative process, with atoms added, bonding established, and the structure minimized in repeated cycles until the desired size structure was obtained (see Fig. 2). We allowed no vacancies in the interior of the individual layers, and the number of 5 and 7 rings were similar to keep the entire sheet relatively flat (this facilitates turbostratic layering). Most of the models were discontinuous at the edge of individual layers; however to evaluate the effect of edge discontinuities and model size, selected models were built with periodic boundaries along one or more edges.

The geometry of the single graphene layer was optimized by energy minimization of the structure using the DREIDING [24] force-field as implemented in Cerius² (Fig. 2). Since the resulting curved structures no longer fit into the classic hexagonal symmetry of graphite—there may be short-range translational order within the sheet, but no long-range periodicity—each 2D graphene sheet of 1000–2000 atoms was treated as a single unit, and artificial ‘unit cell’ parameters **a** and **b** were fit around the graphene sheet. The **a** and **b** dimensions are typically 40–60 Å. The **c** dimension was adjusted to

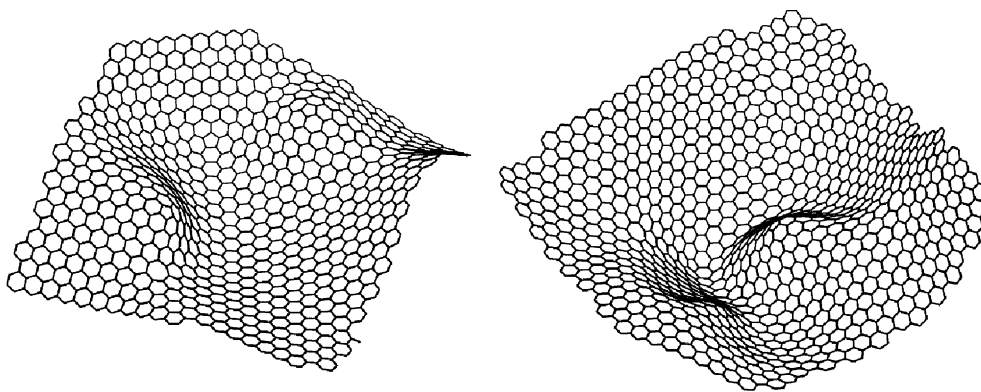


Fig. 2. Models of single layer of graphene sheet created using Cerius² molecular modeling software. Each sheet contains about 1% non-hexagonal rings.

obtain desired model density of 2.2 g/cm^{-3} . In general, the energy minimization of the structures was performed on unconstrained, isolated, non-periodic structures. To approximate how adjacent layers may constrain the shape and atomic positions in individual layers, the energy minimization was repeated on the periodic structure using the ‘unit cell’ defined above.

Three-dimensional model structures were created starting from individual carbon sheets by turbostratically stacking the individual layers, that is, arranging the layers so there exists a small, random displacement in the interlayer spacing. Using DISCUS [25] software, layer-to-layer translations were chosen to reduce interlayer correlations, incorporating random Gaussian deviations in the **a**, **b**, and **c** translations between layers. The fully stacked structure typically consisted of 10 layers; an example structure containing four turbostratically-layered sheets is shown in Fig. 3. The standard deviation of these translational movements was 0.25 \AA . The model PDF was calculated on these 3D structures using DISCUS with maximum scattering vector ($k_{\text{max}} = 40 \text{ \AA}^{-1}$) set to mimic the experimental conditions of the neutron scattering experiments. The atomic displacement parameters (*B* values) were set to fit the height and width of the first two peaks in the PDF of the experimental PFA1200 material. The rationale and implications of this approach are discussed below.

The model PDFs are compared with the experimental data for two samples of pyrolytic carbon prepared from polyfurfuryl alcohol. Quantitative evaluation of the goodness of fit was done using the agreement index or *R*-value [26,27]:

$$R^2 = \frac{\sum_i w_i \cdot [g_{\text{calc}_i} - g_{\text{exp}_i}]^2}{\sum_i w_i \cdot [g_{\text{exp}_i}]^2}$$

where g_i is the $G(r_i)$ at the *i*th point or calculated value in the PDF. The factor is identical to the *R*-value used in

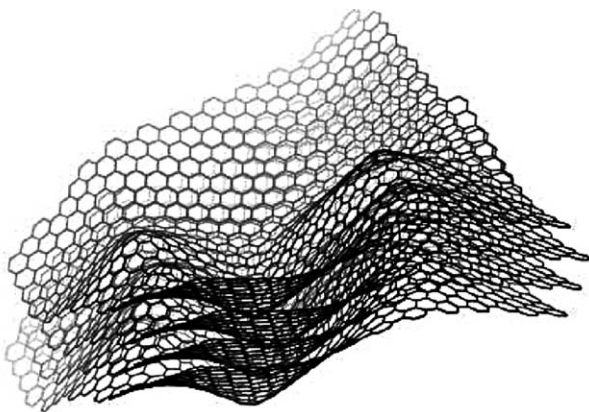


Fig. 3. A model of structure consisting of four turbostratically layered sheets. Models containing typically 10 sheets were used to calculate the PDF.

Rietveld analysis of crystallographic materials, it is a weighted sum of the residuals between experimental and model $G(r_i)$. The weighting factor w_i was set to 1. We employ two different ranges of r in our evaluation, and define R_{0-20} for the range $0-20 \text{ \AA}$, and $R_{4.5-20}$ for the range $4.5-20 \text{ \AA}$. Direct comparisons of the *R*-values calculated over the different ranges is not appropriate due to the different normalization factors. An expected *R*-value may be computed from

$$R_{\text{exp}} = \sqrt{\frac{N - p}{\sum_i w_i \cdot [g_{\text{exp}_i}]^2}}$$

where N is the number of data points and p the number of fit parameters. The ratio of these two statistics gives the standard deviation of the model. Note that other than adjusting atomic displacement parameters to match the first two peaks in the PDF, no iterative fitting of model parameters to experimental data was performed.

3. Results and discussion

The suitability of DREIDING [24] to obtain acceptable bond distances and angles was evaluated by comparing optimized geometry of graphite, C_{60} and C_{70} fullerenes to established values. The results show DREIDING reproduces graphite within-layer bond lengths within 0.0017 \AA . In the carbon models, the accumulated bias error from DREIDING would show as a shift in peak position of less than 0.02 \AA , undetectable within experimental error. For C_{60} , DREIDING under predicts bond length by 0.04 \AA . Such a bias would manifest itself as a shift in peak position of 0.3 \AA at 10 \AA . However, because the model structures contain only $0.5-4\%$ non-hexagonal rings, they more closely resemble graphene sheets than the highly curved C_{60} where 37% of the rings are pentagonal. The graphene result is thus a more meaningful measure of the reliability of the force-field and we conclude that the DREIDING gives results of sufficient accuracy for our purpose.

The key variables that influence the agreement between model and experimental PDF are the selection of an appropriate atomic displacement parameter, the number of non-hexagonal rings in the structure, whether the structure optimization was performed on isolated layers or layers constrained by neighboring layers, the size of the model structures, and the hydrogen content in the material. In what follows we discuss the effect of these variables on the PDF.

The selection of the atomic displacement parameter *B* has a major influence on the fit. This parameter is typically used to capture the peak broadening due to thermal displacement of atoms of their average positions,

where $B = 8\pi^2\langle u^2 \rangle$ is also known as the Debye–Waller parameter, $\langle u^2 \rangle$ represents an average displacement from the atomic position, and the peak broadening follows a Gaussian distribution [10]. We fit the atomic displacement parameter used in model calculations to the first two peaks the PFA1200 data to obtain $B = 0.12 \text{ \AA}^2$. The other key variables primarily affect the PDF at distances outside the first coordination sphere. Thus the selection of atomic displacement parameter is independent of the number of non-hexagonal rings in the structure; the same value of B is achieved using pure graphite as a model. In addition, for model structures with no vacancies, the heights of the first two peaks are identical. This is true for the experimental PFA1200 material, suggesting that our model and approach to estimate B is reasonable. For the PFA800, the data is better modeled using an atomic displacement parameter of $B = 0.35 \text{ \AA}^2$, yet even using this value the difference between the first and second peak height in the experimental PDF is not captured correctly. This suggests that an appropriate model for the nanoporous PFA800 material should include variables not investigated here. We also conclude that using a value of $B = 0.12 \text{ \AA}^2$, we have captured the atomic displacements due essentially to thermal motion. For this value of B , atomic displacement away from an average position is characterized by a standard deviation of $\sigma = 0.05 \text{ \AA}$. This value also results in substantially less broadening for within-layer peaks than layer-to-layer translational dislocations ($\sigma = 0.25 \text{ \AA}$) needed to account for the turbostratic nature of these materials. Because our goal is to use the atomic positions generated by a model building algorithm to understand the inherent disorder in the structure, this value is kept constant throughout the simulation.

Fig. 4 shows the PDF of a series of models containing different fractions of non-hexagonal rings, and the PDF of the two experimental samples. The similarity between the PFA1200 data with the model containing 1.0% non-hexagonal rings is remarkable. These results are highly reproducible: similar patterns are obtained with other models of similar size and similar fraction of non-hexagonal rings. The agreement indices are shown in Table 1. We report the agreement indices over two different

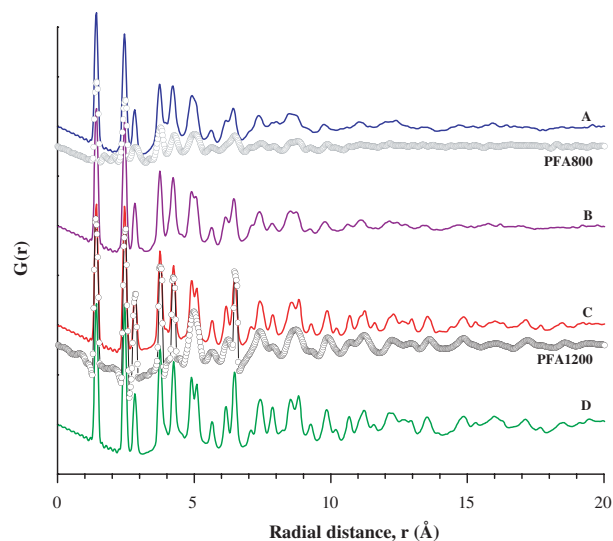


Fig. 4. Atomic pair distribution functions of two experimental materials PFA1200 and PFA800, with calculated PDF of four model structures of turbostratically layered graphene sheets with $A = 3.9\%$, $B = 2.8\%$, $C = 1.0\%$, and $D = 0.5\%$ non-hexagonal rings.

ranges of the radial distance r : first, for the data from 0 to 20 Å, and then considering only the data with r from 4.5 to 20 Å, that is, outside the first five nearest neighbors. Also shown are the expected agreement indices, note that the ratio of R/R_{exp} is the standard deviation of the model. It is evident from Table 1 that the model with 1% non-hexagonal rings fits best the PFA1200 PDF, the standard deviation is 0.28 over the range of r from 0 to 20 Å. The PDF for PFA800 is best fit by the model structure with 4% non-hexagonal rings; however, the agreement is still poor. This is certainly in part due to factors not accounted for in our studies, but also because the denominator of the R -value is a measure of the information density in the PDF. Since there is less structural information in the experimental PDF of PFA800, the larger agreement indices reflect that there is greater uncertainty in the fit of the model to a real structure. The following discussion centers on models with 1% non-hexagonal rings and the PFA1200 pyrolytic carbon.

Table 1

Agreement indices (R -value) for model structures with differing fraction of non-hexagonal rings and experimental PDF of two samples of carbon prepared from the pyrolysis of polyfurfuryl alcohol

Fraction of non-hexagonal rings	Fit to PFA1200 data		Fit to PFA800 data	
	$r = 0-20 \text{ \AA}$	$r = 4.5-20 \text{ \AA}$	$r = 0-20 \text{ \AA}$	$r = 4.5-20 \text{ \AA}$
3.90%	0.27	0.56	0.95	2.17
2.80%	0.19	0.43	1.19	2.78
1%	0.14	0.32	1.98	6.14
0.50%	0.15	0.44	2.34	9.35
Expected R	0.46	1.00	1.22	3.60

Note that ratio of R -value to expected R -value is standard deviation of model.

For all model structures, the optimization was first performed on a single sheet in free space, unconstrained by any boundaries or neighboring layers. Thus, the local curvature of any sheet is affected only by the number and location of 5- and 7-member rings. It is expected, however, that the local curvature of any sheet is also affected by neighboring layers. This effect is approximated by carrying out additional structural minimization with periodic boundaries in the *c* direction. Fig. 5 shows how this constrained structure optimization affects the model appearance and PDF. There is a small change in the agreement between model and experimental PDFs: the fit is overall poorer but improves for *r* between 4.5 and 20 Å. From the figures, the effect of the constrained structure optimization is to accentuate the curvature along the borders between non-hexagonal rings; the individual peaks and valleys are sharper. Such sharp corners are observed in HRTEM images of very high temperature pyrolytic carbons and fullerene-like onion structures [9,22]. Furthermore, as in PFA1200 where the density approaches that of graphite, it is expected that adjacent layers will influence geometry. Therefore, despite that DREIDING nor other simple force-field accurately predicts the interlayer forces in graphite accurately, the constrained minimizations give the right trend when modeling high-temperature pyrolytic and glassy carbons.

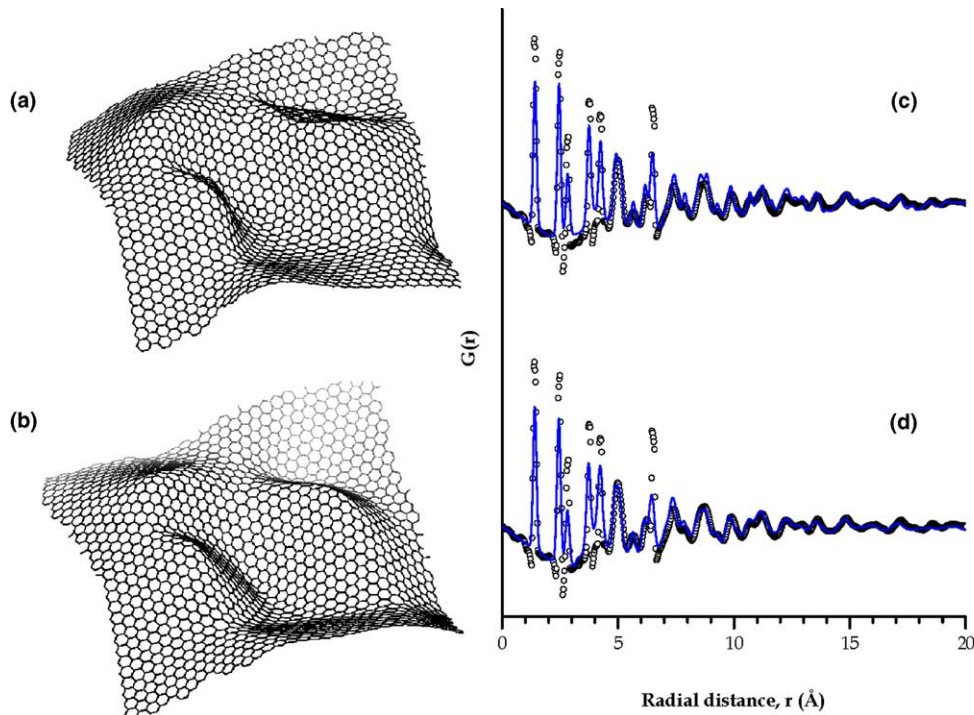


Fig. 5. (a) Model obtained with structure optimization not constrained by adjacent layers; (b) same model with structure optimization performed with adjacent layers in place to mimic effect of layer spacing. Note the sharper features relative to (a); (c) PDF of structure developed with unconstrained structure optimization; and (d) same structures with constrained optimization. The model PDFs (line) overlay the PFA1200 experimental data (open circles).

The effect of the edges and size of the individual fragments manifests itself in a way similar to curvature generated by non-hexagonal rings. The effect of model size at a constant 1% fraction of non-hexagonal rings is illustrated in Fig. 6. Qualitatively, for example, the

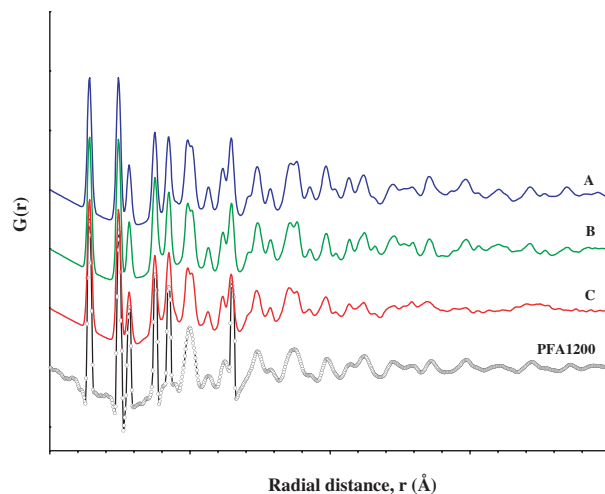


Fig. 6. Calculated PDF of three model structures each with 1.0% non-hexagonal rings of different sizes: *A* = an infinitely repeating sheet, *B* = 1200 atoms, and *C* = 400 atoms. Shown with experimental PDF PFA1200.

structure with only 400 atoms ($30 \times 30 \text{ \AA}$) is not satisfactory especially in the range from 10–20 \AA , while the structures with 1200 atoms ($50 \times 50 \text{ \AA}$) and an infinitely repeating structure show little difference. Thus we conclude that a model composed of 1200–2000 carbon atoms is sufficiently large to effectively eliminate edge effects.

Investigations by Franklin [2] and others [3,5,7,12] frequently described the structure of non-graphitizing carbons in terms of a *c*-axis correlation length, L_c , and a basal plane correlation length, L_a . The long-range disorder was modeled by a distribution of L_a , corresponding to graphene fragments of different size or with different number of rings in one fragment. Franklin concluded that non-graphitizing carbons consisted of graphitic microdomains of $L_a = 16 \text{ \AA}$, and $L_c = 5 \text{ \AA}$, essentially single layers of roughly 100 atoms. Similarly, Claye and Fisher [7] studied carbons derived from epoxy resin pyrolyzed at less than 1000 °C and concluded these materials are best modeled by a collection of single layer graphene fragments with a lateral dimension of 10 \AA . The fraction of non-hexagonal rings in our models may be qualitatively related to the intraplane correlation length L_a . Consider a small, circular section of 200 carbon atoms (~ 100 rings) in a single sheet with one non-hexagonal ring. Since the hexagonal tiling dominates, the approximate area of such a section will be $\sim 524 \text{ \AA}^2$. For any single carbon atom, the correlation length can be thought of as the average distance to the nearby non-hexagonal ring (beyond which the structure is essentially uncorrelated), or for a circular section, about 13 \AA . This compares favorably with results reported by Franklin and Claye et al. The dimension of the model containing 1200 °C atoms is about $50 \times 50 \text{ \AA}$, substantially larger than the correlation lengths found by other researchers, thus reinforcing our conclusion it is not model size, but rather the curvature generated by non-hexagonal rings within a graphene sheet and that accounts for the fit of model to experimental PDF.

Nanoporous carbons created from pyrolysis of polymers contain hydrogen, the hydrogen content being a function of pyrolysis temperature (for the two materials under consideration here it is reasonable to assume the amount of other heteroatoms is negligible) [17]. For the PFA1200 carbon, the H/C ratio is expected to be 0.03. We investigated the impact of hydrogen in our models by allowing hydrogen to fill the dangling bonds at the disconnected edges of our model graphene sheets. This approach overestimates the H/C ratio (for a 1200 carbon atom model, H/C = 0.8), and resulting PDF do not fit the experimental data as well as a pure-carbon model. Moreover, we were not able to justify this method of incorporating hydrogen into the structure other than convenience. Despite that the effect of hydrogen on the PDF is important, no conclusions can

be drawn about the nature and location of hydrogen in pyrolytic carbons.

As was emphasized at the outset, scattering data reveals little information about the relationship between adjacent layers; that is, there are no features in the PDF that are attributable to scattering between atoms in different layers. This turbostratic nature of these carbons means that all of the structural information available from any diffraction study can be modeled in a two-dimensional sheet. The three-dimensional structures we create are constructs needed to facilitate calculation of the PDF, and are not precise models of actual materials. The most serious limitation of the 3D, multi-layered structure as models of real carbons is that they are anisotropic, in marked contrast to the well-documented isotropic nature of non-graphitizing carbons [2,3,5,6,17]. Real glassy carbon structures likely contain domains that overlap only in part; where overlap occurs, the curvature of adjacent layers would be similar but not necessarily identical. Furthermore, there is no reason to expect the number of 5- and 7-member rings to be the same (this was done to ensure the turbostratic layering would not result in intersecting layers). More realistically, regions of similar curvature result in interlocking pockets and intertwined sections. Further work will be required to develop fully realistic three-dimensional models that have intertwined cusped and saddled surfaces that would mimic an intertwined layered non-graphitic carbon structure. Information on the relationship between different layers will have to be obtained from something other than the PDF as, as shown here and elsewhere, the PDF effectively only captures atomic structure within one layer.

As noted above the models with up to 4% non-hexagonal rings do not adequately describe the PDF of PFA800: there are better-defined peaks in the model PDF than observed in the experimental PDF. There is very little structural information in the experimental PDF for distances 5–12 \AA , and essentially none for $r > 12 \text{ \AA}$. This suggests other forms of disorder in the 800 °C carbon—for example, vacancies, the presence of residual heteroatoms of oxygen or crosslinking sp^3 carbon—should be added to the model. Moreover, the lack of information in the experimental PDF of the 800 °C carbon means there may be many plausible structures with the same calculated PDF. Therefore, other techniques and sources of information are needed to pinpoint the details of the structure of these materials.

We have shown that a simple model composed of layered sheets of sp^2 carbon and altered by the presence of a small fraction of 5- and 7-member rings has a PDF remarkably similar to the experimental PDF of carbon prepared from the 1200 °C pyrolysis of polyfurfuryl alcohol. We showed that the most important variable in the model is the fraction of non-hexagonal rings. The effect of other variables with a significant impact of the

PDF such as atomic displacement parameter and structure optimization were evaluated, and the methodology used to estimate values for these variables is chemically and physically reasonable. We showed that edge or size effects in our models are not significant, we related the fraction of non-hexagonal rings to the L_a correlation length used by earlier researchers to describe similar non-graphitizing carbons. We emphasize that no effort was made to ‘fit’ model to the experimental data: we create the structures, calculate the PDF and examine the correspondence between model and experiment. Despite the model’s oversimplified structure, developed to facilitate calculation of the PDF, the individual layers provide a good approximation of the fraction of non-hexagonal rings in the non-graphitic carbon and are good starting models for the simulation of these important materials.

Acknowledgements

We would like to thank Valeri Petkov for kindly sharing his PDF data. The work was funded by a grant from the Camille and Henry Dreyfus Foundation, and NFS grant EEC-0085461.

References

- [1] Warren B. X-ray diffraction in random layer lattices. *Phys Rev* 1941;59(9):693–8.
- [2] Franklin RE. Crystallite growth in graphitizing and non-graphitizing carbons. *Proc Roy Soc London Series A—Math Phys Sci* 1951;209(1097):196–218.
- [3] Robertson J. Amorphous-carbon. *Adv Phys* 1986;35(4):317–74.
- [4] Foley HC. Carbogenic molecular sieves: synthesis, properties and applications. *Micropor Mater* 1995;4:407–33.
- [5] Harris PJF. Structure of non-graphitising carbons. *Int Mater Rev* 1997;42(5):206–18.
- [6] Foley HC, Kane MS. Local microstructural organization in carbogenic molecular sieves. In: *Materials Research Society Symposium*. Materials Research Society; 1996;431:9–14.
- [7] Claye A, Fischer JE. Short-range order in disordered carbons: where does the Li go? *Electrochim Acta* 1999;45(1–2):107–20.
- [8] Praver S, Rossouw CJ. Structural investigation of helium ion-beam-irradiated glassy-carbon. *J Appl Phys* 1988;63(9):4435–9.
- [9] Harris PJF, Tsang CJ. High-resolution electron microscopy studies of non-graphitizing carbons. *Philos Mag A—Phys Condensed Matter Struct Defects Mech Prop* 1997;76(3):667–77.
- [10] Warren BE. X-ray diffraction. New York: Dover Publications; 1990. vii, 381 p.
- [11] Billinge SJL, Thorpe MF. Local structure from diffraction. In: *Fundamental materials research*. New York: Plenum Press; 1998. x, 399 p.
- [12] Thomson KT, Gubbins KE. Modeling structural morphology of microporous carbons by reverse Monte Carlo. *Langmuir* 2000; 16(13):5761–73.
- [13] Green DC, Mckenzie DR, Lukins PB. The microstructure of carbon thin films. *Mater Sci Forum* 1989;52&53:103–24.
- [14] Gardner MA et al. Structural studies of microporous carbons by neutron diffraction. *Carbon* 1996;34(7):857–60.
- [15] Burian A et al. Radial distribution function analysis of the structure of activated carbons. *Carbon* 1998;36(11):1613–21.
- [16] Petkov V et al. Local structure of nanoporous carbons. *Philos Mag B—Phys Condensed Matter Statist Mech Electron Opt Magn Prop* 1999;79(10):1519–30.
- [17] Foley HC, Kane MS, Goellner JF. Access in nanoporous materials. In: *Symposium on Access in Nanoporous Materials*, Michigan State University, East Lansing, Michigan, June 7–9, 1995. Plenum Press; 1995;39–58.
- [18] Mackay AL, Terrones H. Diamond from graphite. *Nature* 1991; 352(6338):762.
- [19] Terrones H, Mackay AL. The geometry of hypothetical curved graphite structures. *Carbon* 1992;30(8):1251–60.
- [20] Mackay AL, Terrones H. Hypothetical graphite structures with negative Gaussian curvature. *Philos Trans Roy Soc London Series A—Math Phys Eng Sci* 1993;343(1667):113–27.
- [21] Townsend SJ et al. Negatively curved graphitic sheet model of amorphous-carbon. *Phys Rev Lett* 1992;69(6):921–4.
- [22] Bourgeois LN, Bursill LA. High-resolution transmission electron microscopic study of nanoporous carbon consisting of curved single graphitic sheets. *Philos Mag A—Phys Condensed Matter Struct Defects Mech Prop* 1997;76(4):753–68.
- [23] Cerius² modeling environment. 1997, Molecular simulations: San Diego.
- [24] Mayo SL, Olafson BD, Goddard WA. Dreiding—a generic force-field for molecular simulations. *J Phys Chem* 1990;94(26):8897–909.
- [25] Proffen T, Neder RB. DISCUS: a program for diffuse scattering and defect-structure simulation. *J Appl Crystallogr* 1997;30:171–5.
- [26] Proffen T, Billinge SJL. PDFFIT, a program for full profile structural refinement of the atomic pair distribution function. *J Appl Crystallogr* 1999;32:572–5.
- [27] Peterson PF et al. Improved measures of quality for the atomic pair distribution function. *J Appl Crystallogr* 2003;36: 53–64.